nature communications

Article

https://doi.org/10.1038/s41467-025-57891-7

Ecological restoration in the Yellow River Basin enhances hydropower potential

Received: 11 September 2024

Accepted: 5 March 2025

Published online: 15 March 2025

Check for updates

Xutong Wu[1], Zihan Yan[2], Haiyan Yang[2], Shuai Wang[1] ✉, Haoyu Zhang[1], Yilin Shen[3], Shuang Song[1], Yanxu Liu[1], Ying Guo[3], Dawen Yang[2] & Bojie Fu[4]

Hydropower, an important renewable energy source worldwide, is threatened by reservoir sedimentation. Ecological restoration (ER) can mitigate this by reducing upstream sediment, thereby extending hydropower facilities' lifespan. However, ER may also reduce runoff, potentially diminishing energy generation and complicating its overall impact on hydropower potential. Here, we examine China's Yellow River, once the world's most sediment-laden river, using eco-hydrological and reservoir regulation models to assess how large-scale ER influences the hydropower potential of the Xiaolangdi Reservoir, which controls 92.3% of the basin area. Our results indicate that, excluding upstream reservoirs' operations and socioeconomic water use, Xiaolangdi could generate a total of ~2.7×10^{11} kWh of energy before facing diminished flexibility and efficiency caused by the exhaustion of sediment storage—57.3% more than without ER—equating to an additional ~100 billion kWh. This enhancement in hydropower potential primarily arises from the extended lifespan, despite a 6.9% reduction in average annual energy generation. These findings advance our understanding of the ecosystem-water-sediment-energy nexus, offering valuable insights for integrated watershed management globally.

Ensuring access to affordable and clean energy is essential for achieving the Sustainable Development Goals[1], necessitating a substantial increase in the share of renewable energy, such as hydro, solar, and wind. Hydropower has been the leading renewable energy source worldwide, with a total capacity of 1,268 GW by the end of 2023, accounting for 14% of global installed power capacity and 33% of global renewable power capacity[2]. In the transition to a net-zero emissions energy system, hydropower offers a cost-effective alternative to the high solar and wind installation costs at the current technological level[3]. Its flexibility and energy storage capacity can effectively balance the intermittent supply from solar and wind sources and meet peaks in energy demand on grids[4–6]. Consequently, hydropower has experienced renewed interest and rapid expansion in recent decades[7], with an unprecedented 75% growth from 2000 to 2021[8], particularly in Asia-Pacific, South America, and Africa[9]. Nevertheless, vast untapped hydropower potential remains[10], with considerable expansion planned or underway in the Global South[11].

Despite being the most mature renewable technology, hydropower faces significant challenges, notably reservoir sedimentation. Sedimentation impairs reservoir's storage capacity and abrades power turbines[12], undermining the longevity of reservoirs and diminishing the operational flexibility of hydropower generation. Without adequate storage, hydropower facilities become reliant on seasonal flows, which might not occur when energy is needed, thus negating one of the primary advantages of hydropower over other renewable energy sources. Reservoirs worldwide lose approximately 0.5–1% of their initial storage

[1]State Key Laboratory of Earth Surface Processes and Hazards Risk Governance, Faculty of Geographical Science, Beijing Normal University, Beijing, China. [2]State Key Laboratory of Hydroscience and Engineering, Department of Hydraulic Engineering, Tsinghua University, Beijing, China. [3]CAS-Key Laboratory of Agricultural Water Resources, Hebei-Key Laboratory of Water Saving Agriculture, Center for Agricultural Resources Research, Institute of Genetics and Developmental Biology, Chinese Academy of Sciences, Shijiazhuang, China. [4]State Key Laboratory of Regional and Urban Ecology, Research Center for Eco-Environmental Sciences, Chinese Academy of Sciences, Beijing, China. ✉e-mail: shuaiwang@bnu.edu.cn

capacity annually due to sedimentation[13]. A study of over 47,000 dams across 150 countries revealed that these dams had already lost 16% of their combined original storage capacity by 2022 due to trapped sediment, with this figure expected to rise to 26% by 2050[14]. The higher erosion rates and increased sediment load caused by climate change and changes in watershed land use are likely to exacerbate reservoir sedimentation issues faster than previously anticipated[15,16], amplifying the threat to the sustainability of hydropower.

Watershed land use management to control soil erosion can effectively mitigate reservoir sedimentation from upstream sources[17]. Vegetation measures, such as afforestation and grass planting, mitigate erosion by enhancing infiltration and reducing overland flows[18,19], while engineering measures, such as terraces and check dams, decrease discharge velocity and increase surface storage, thereby reducing sediment transport[19,20]. These measures can extend the operational lifespan of hydropower facilities by reducing sediment flows into reservoirs[18]. However, large-scale afforestation often increases evapotranspiration (ET), leaving less water for runoff[21]—especially in semiarid and arid regions[22]—thereby diminishing hydropower potential, which depends directly on streamflow[23]. These opposing effects through changes in sediment and runoff raise an elusive question: what is the net impact of watershed land use management on hydropower potential? Existing studies typically focus on the separate effects through runoff or sediment change[23,24] or seek future optimal management strategies by simultaneously considering these effects[25,26]. However, research integrating these opposing effects to analyze how real-world practices affect hydropower potential remains limited.

To address this knowledge gap, we select China's Yellow River (YR) to explore how large-scale ecological restoration (ER) in the Yellow River Basin (YRB) affects the hydropower potential of the Xiaolangdi Reservoir, a strategic water conservancy project in the YR controlling 92.3% of the total basin area (Fig. 1a). The YR is an ideal case for this research, as it once carried the largest sediment load of any river in the world[27,28]. Severe sedimentation problems plagued its first dam, the Sanmenxia Reservoir, which lost more than 40% of its storage capacity within the first four years and underwent extensive reconstruction afterward[29]. To address the sediment issue, numerous soil and water conservation practices have been implemented since the 1970s, including terracing, check dam construction, and vegetation restoration[20] (Supplementary Fig. 1). Among them, the Grain-for-Green Program (GFGP) implemented since 1999 is the largest and most successful[30]. Vegetation coverage of the YRB has significantly increased since 2000 (Fig. 1a), leading the greening process of China[31]. Along with these ER measures, the sediment load and streamflow of the YR have significantly decreased[20] (Fig. 1b, c). The Xiaolangdi Reservoir, completed in 2001, has a total installed capacity of 1800 MW[32]. It has a total storage capacity of 12.65 billion m^3, including a sediment storage capacity of 7.55 billion m^3 for sediment deposition and a regulating storage capacity of 5.10 billion m^3 for flow regulation and electricity generation[32] (Supplementary Fig. 2). The operating period of the Xiaolangdi Reservoir coincides with the implementation of large-scale ER in the YRB, providing an excellent opportunity to analyze the overall impact of ER on its hydropower potential by affecting the sediment and runoff of the YR.

In this study, we use the designed sediment storage capacity of the Xiaolangdi Reservoir as a benchmark to evaluate total energy generation. Once this storage is filled, regulating storage is invaded, compromising the flexibility and efficiency of hydropower. Total energy generation is determined by monthly energy production and the sediment storage lifespan. As previously noted, energy production depends positively on reservoir inflow, while sediment storage lifespan depends inversely on sediment load. These factors are influenced by upstream land use, climate, socioeconomic water use, and reservoir operations. To isolate the impact of ER on hydropower potential, we design an idealized experiment simulating streamflow and sediment load of the YR under two scenarios: with and without ER implementation (2000–2019), while holding other influencing factors consistent. Both simulations use observed meteorological data to reflect climate variability, with upstream socioeconomic water use and reservoir operations excluded (Methods, Supplementary Table 1). The Geomorphology-Based Eco-Hydrological Model with Soil and Water Conservation (GBEHM-SWC), a distributed model that integrates the complex eco-hydrological interactions and human interferences in the YRB (Supplementary Fig. 3), is employed to simulate eco-hydrological and sediment dynamics. We then simulate the regulation of the Xiaolangdi Reservoir and its energy generation and sedimentation processes, comparing the total generated energy under both scenarios. By revealing the impact of ER in the YRB on the hydropower potential of the Xiaolangdi Reservoir, this study advances understanding of the ecosystem-water-sediment-energy nexus and provides valuable insights for integrated watershed management.

Results

Hydrological and sediment responses to ecological restoration

According to the Soil and Water Conservation Bulletin in Yellow River Basin[33], by 2020, extensive ER measures had been implemented in the YRB, including the establishment of 12.64×10^4 km^2 of forests, 6.08×10^4 km^2 of terraces, 2.34×10^4 km^2 of grasses, and 5.81×10^4 check dams (Supplementary Figs. 4 and 5). These measures led to significant increases in leaf area index (LAI) and gross primary productivity (GPP) across the basin (Fig. 2). Under the scenario with ER, the basin-averaged LAI from 2000 to 2019 increased by 6.33×10^{-2} m^2 m^{-2} (a relative change of +10.78%) compared to the scenario without ER, while GPP increased by 47.50 g C m^{-2} (+13.04%). Notably, the differences between the two scenarios expanded over time. ER also effectively mitigated soil erosion, with basin-averaged erosion from 2000 to 2019 declining by 706.74 t km^{-2} (−57.11%). However, the large-scale implementation of ER increased basin-averaged ET by 11.39 mm (+3.02%), resulting in a corresponding reduction in basin-averaged runoff by 8.32 mm (−11.02%).

These eco-hydrological changes in the YRB caused by ER have led to significant reductions in both streamflow and sediment load of the YR (Fig. 3). Simulations indicate that, under the scenario with ER, the average annual streamflow into the Xiaolangdi Reservoir from 2000 to 2019 was 401.35×10^8 m^3, a 7.9% decrease from the 435.82×10^8 m^3 observed under the scenario without ER (Fig. 3a). The reduction in average annual sediment load was even more pronounced, falling from 7.54×10^8 t to 4.61×10^8 t, a reduction of 38.9% (Fig. 3c). With the implementation of ER measures, the disparity in streamflow and sediment load between the scenarios with and without ER widened significantly (Fig. 3b, d), showing an average reduction of 53.60×10^8 m^3 (−11.7%) in streamflow and 3.28×10^8 t (−42.3%) in sediment load during the last five years (2015–2019).

Changes in energy generation and sedimentation of the Xiaolangdi Reservoir

Based on the simulated hydrological and sediment conditions of inflow into the Xiaolangdi Reservoir under different scenarios, we further simulated and compared the reservoir's potential energy generation and sedimentation from 2002 onwards (Fig. 4), following the completion of construction at the end of 2001. The average annual energy generation from 2002 to 2019 under the scenario with ER was 121.00×10^8 kWh, a 6.9% decrease from the 130.01×10^8 kWh generated under the scenario without ER. The energy generation process and differences between the two scenarios exhibited intra-annual variation, with June to November contributing more than 60% of the annual energy generation under both scenarios. August and September showed the largest declines in monthly energy generation under the scenario with ER, with reductions of 17.8% and 11.5%, respectively. The average annual reservoir sedimentation also decreased with ER

https://doi.org/10.1038/s41467-025-57891-7

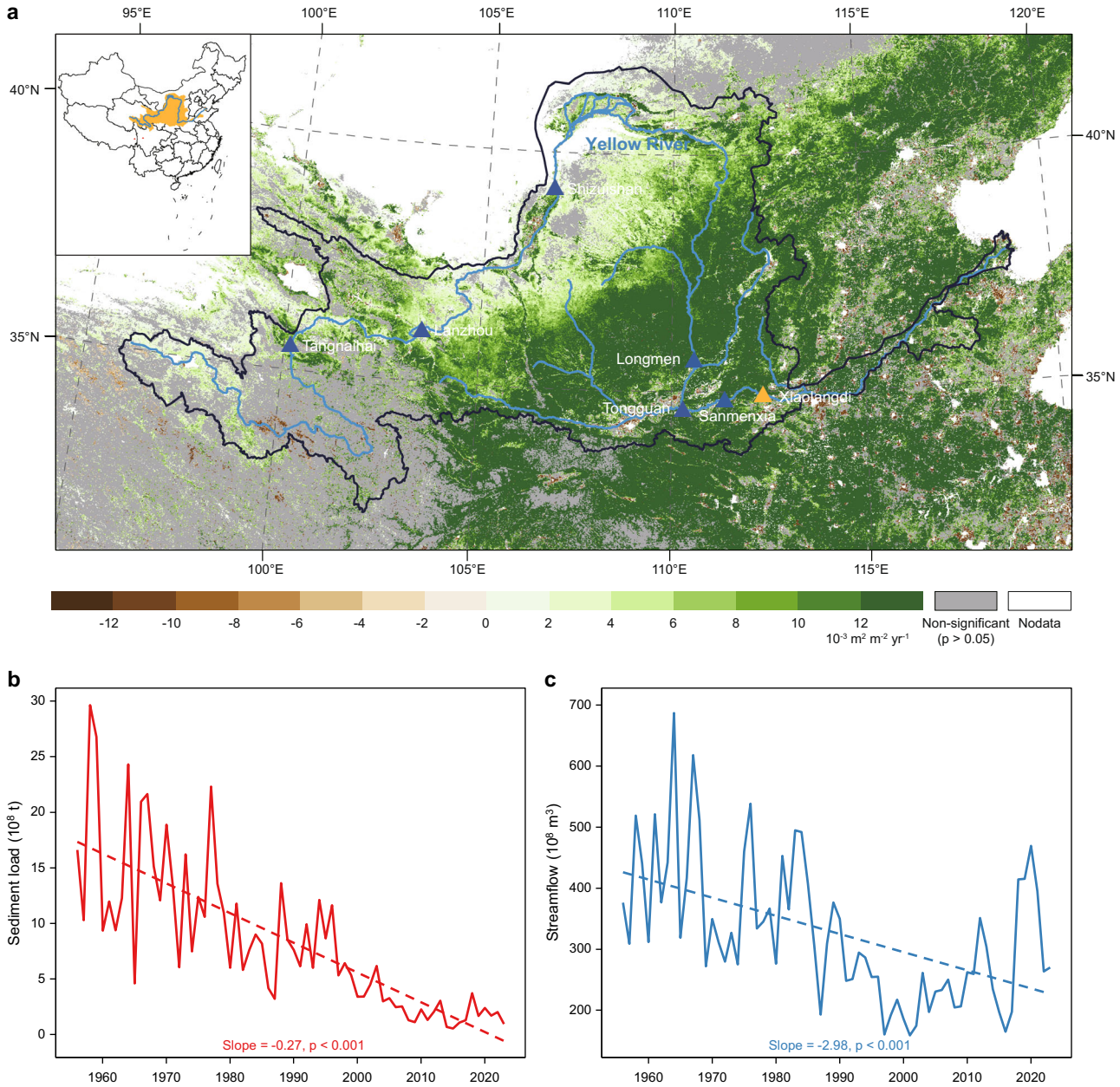

Fig. 1 | Location of the Yellow River Basin and changes in vegetation, sediment load, and streamflow. a Annual moderate resolution imaging spectroradiometer (MODIS) leaf area index (LAI) trend for the entire basin from 2000 to 2023. **b**, **c** Annual sediment load and streamflow at the Tongguan station from 1956 to 2023.

implementation, reducing from 5.44×10^8 m^3 under the scenario without ER to 3.36×10^8 m^3 under the scenario with ER, a decline of 38.3%. The flood season, spanning May to October, accounted for more than 90% of the annual sedimentation under both scenarios, with July and August contributing the most. The largest declines in monthly reservoir sedimentation under the scenario with ER also occurred in July and August, with reductions of 51.5% and 47.0%, respectively.

Accumulated energy generation enhanced by ecological restoration

Although the Xiaolangdi Reservoir exhibited higher average annual energy generation under the scenario without ER, the accompanying higher reservoir sedimentation significantly shortened the reservoir's sediment storage lifespan compared to the scenario with ER (Fig. 5). The accumulated reservoir sedimentation under the scenario without ER was 97.91×10^8 m^3 by December 2019, the endpoint of our simulation. Using the designed sediment storage capacity of the Xiaolangdi Reservoir, 75.50×10^8 m^3, as the threshold for the reservoir's lifespan, the sedimentation reached 75.90×10^8 m^3 in July 2015, thereby exhausting the sediment storage capacity. The total energy generation under this scenario was 1713.63×10^8 kWh. However, under the scenario with ER, the accumulated reservoir sedimentation was only 60.43×10^8 m^3 by December 2019, utilizing just 80% of the sediment storage capacity. Despite lower average annual energy generation, the accumulated energy generation under the scenario with ER exceeded that of the scenario without ER in May 2016, reaching 2177.96×10^8 kWh by December 2019. According to the trend derived from our simulation, the sediment storage capacity of the Xiaolangdi Reservoir under the scenario with ER would be exhausted in 2024, with a total energy generation of 2694.89×10^8 kWh, 57.3% higher than the scenario without ER, providing approximately 100 billion kWh of additional energy.

https://doi.org/10.1038/s41467-025-57891-7

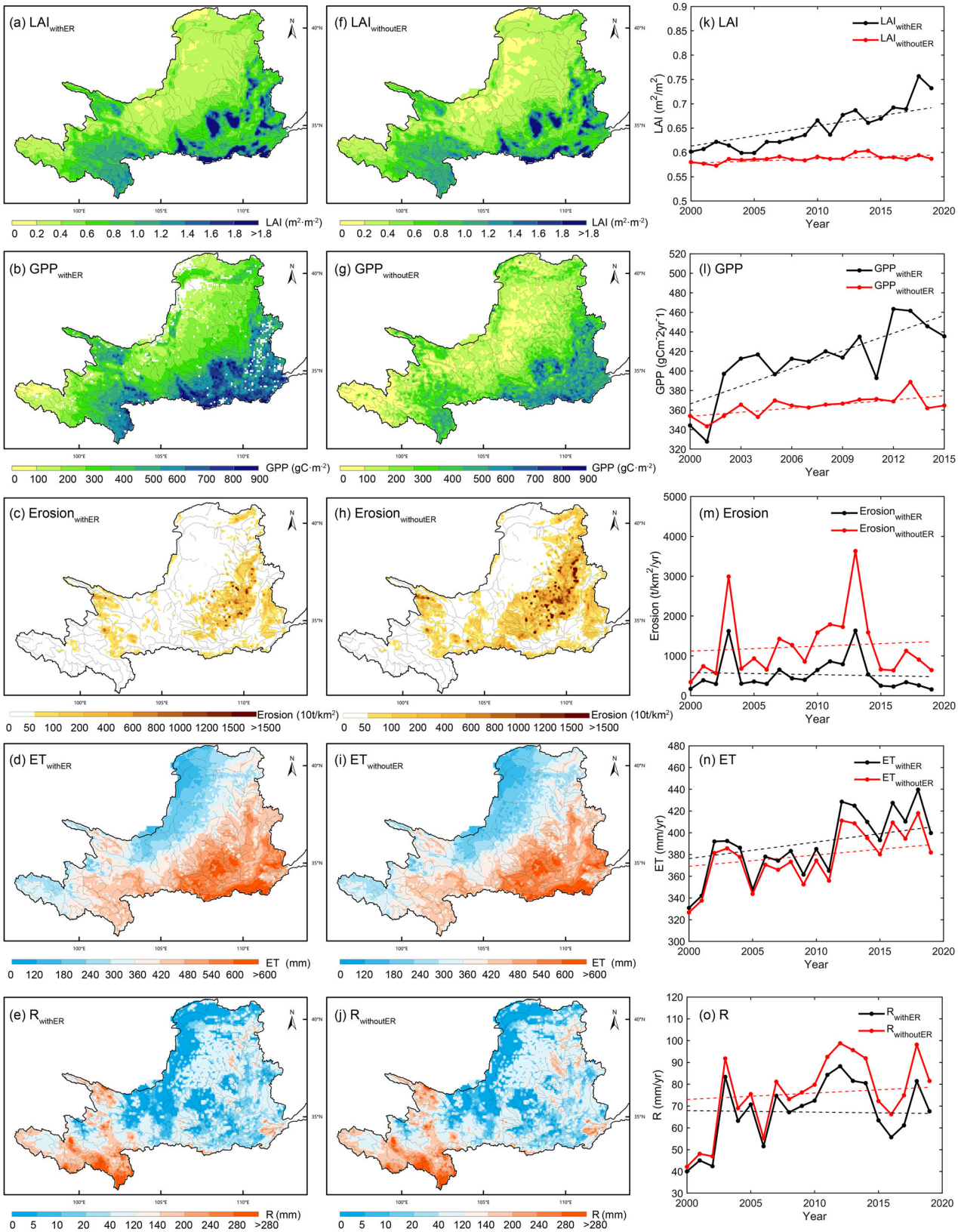

Fig. 2 | Changes in leaf area index (LAI), gross primary productivity (GPP), soil erosion, evapotranspiration (ET), and runoff (R) in the Yellow River Basin under scenarios with and without ecological restoration. **a**–**e** Maps of the average values of these variables from 2000 to 2019 under the scenario with ecological restoration. **f**–**j** Maps of the average values of these variables from 2000 to 2019 under the scenario without ecological restoration. **k**–**o** Changes in the basin-average values of these variables from 2000 to 2019 under the two scenarios.

https://doi.org/10.1038/s41467-025-57891-7

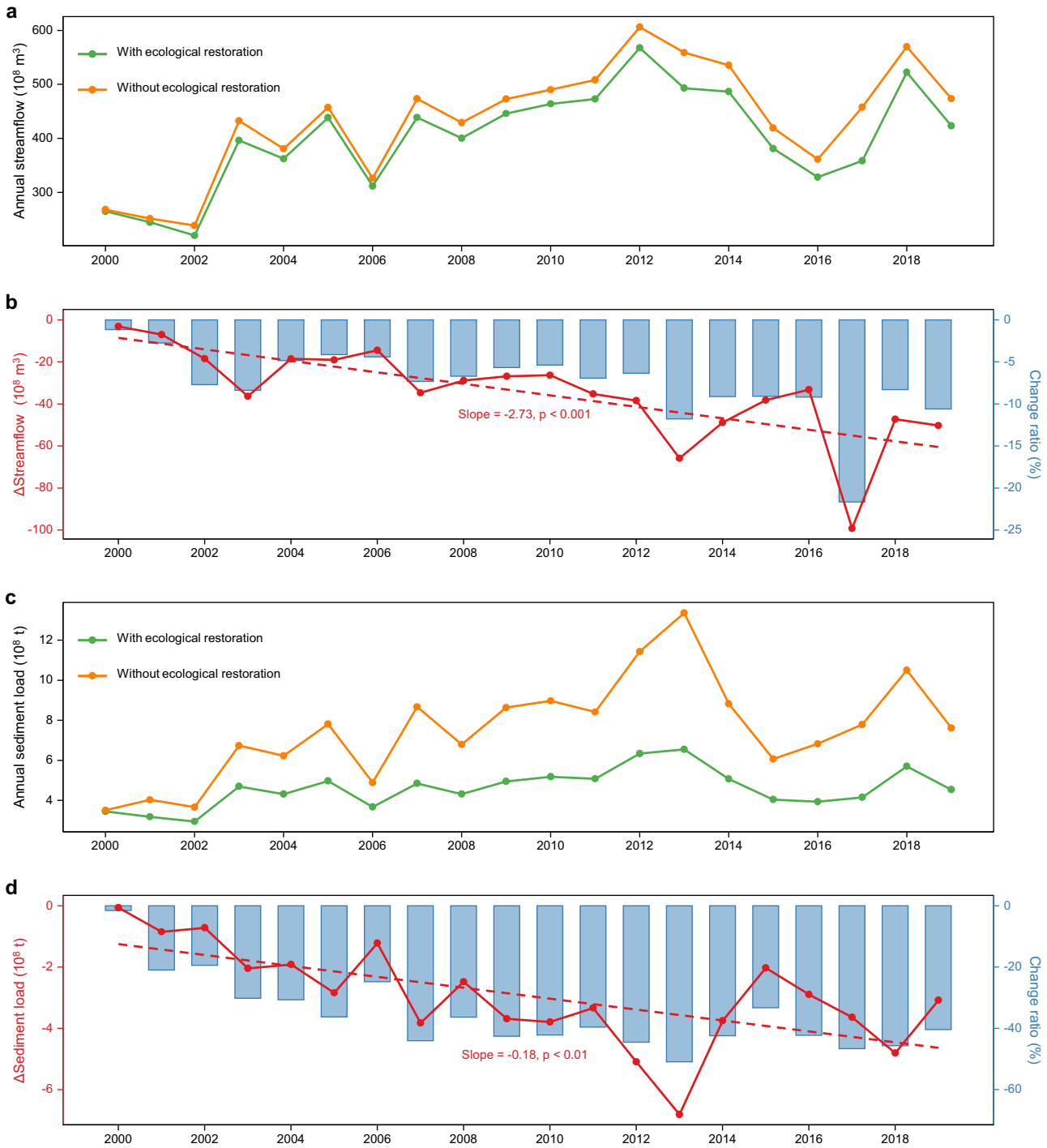

Fig. 3 | Streamflow and sediment load into the Xiaolangdi Reservoir from 2000 to 2019 under scenarios with and without ecological restoration, and the differences between them. a Streamflow from 2000 to 2019. **b** Differences in streamflow between the two scenarios. **c** Sediment load from 2000 to 2019. **d** Differences in sediment load between the two scenarios.

Discussion

Integrating the opposing effects through sediment and runoff changes to understand the overall impact of ER on hydropower potential is crucial for effective watershed management. Utilizing eco-hydrological and reservoir regulation models, our study revealed that ER in the YRB enhances the hydropower potential of the Xiaolangdi Reservoir. Compared to the scenario without ER, the scenario with ER exemplifies the proverb "slow and steady wins the race": despite a 6.9% reduction in average annual energy generation due to decreased streamflow, the reduced sediment load prevents the premature loss of regulating storage capacity, preserving the flexibility and efficiency of energy generation and ultimately providing an additional ~100 billion kWh of energy.

The observed enhancement of hydropower potential due to ER deepens our understanding of the ecosystem-water-sediment-energy nexus. The GFGP and other ER measures in the YRB have significantly increased vegetation coverage and improved multiple ecosystem services, such as carbon sequestration and soil conservation[20,34], while reducing sediment load and improving water quality of the YR[35]. However, vegetation restoration has also led to soil moisture decline

https://doi.org/10.1038/s41467-025-57891-7

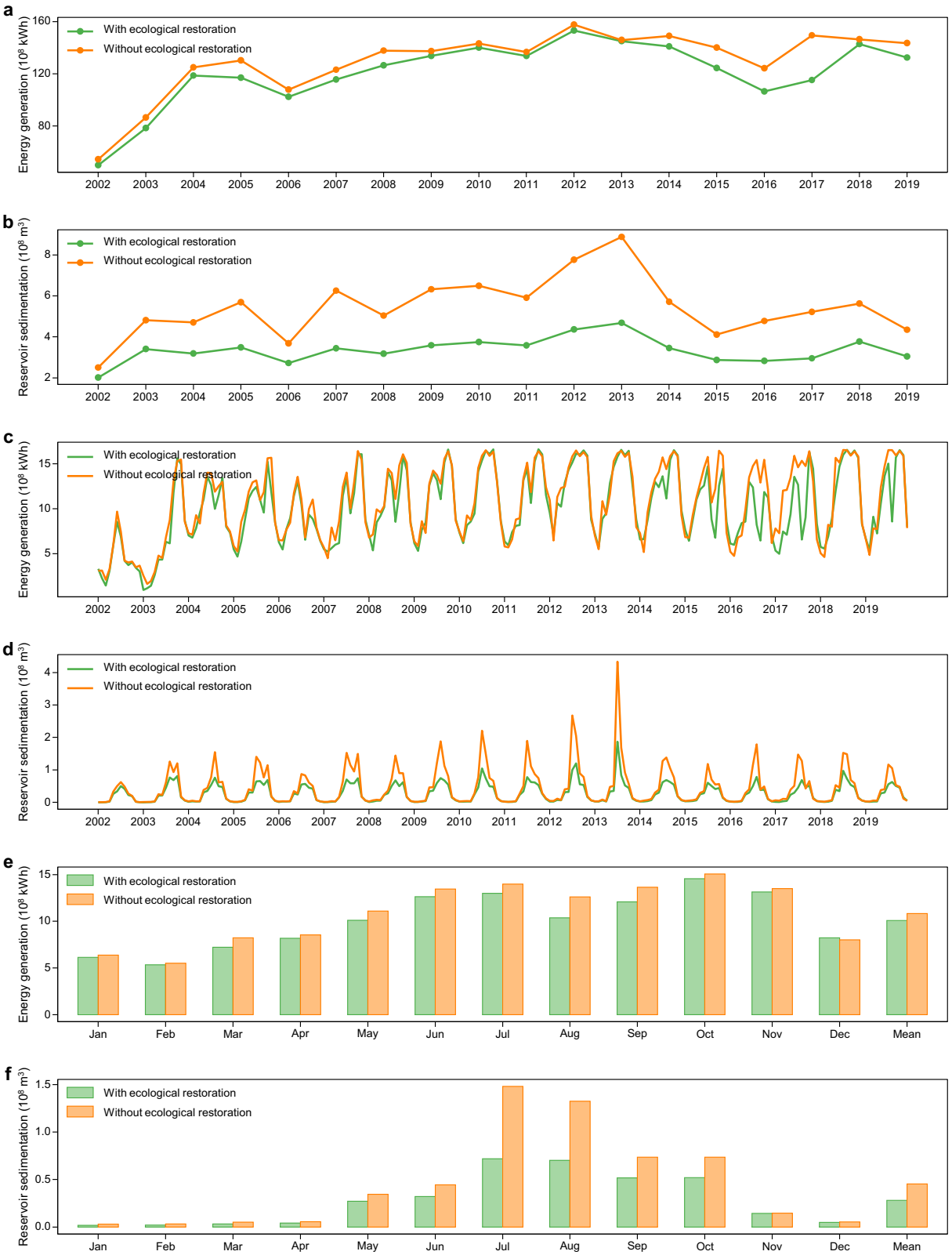

Fig. 4 | Annual and monthly energy generation and sedimentation of the Xiaolangdi Reservoir from 2002 to 2019 under scenarios with and without ecological restoration, and comparison of their mean values. a Annual energy generation from 2002 to 2019. **b** Annual sedimentation from 2002 to 2019. **c** Monthly energy generation from 2002 to 2019. **d** Monthly sedimentation from 2002 to 2019. **e** Comparison of average monthly energy generation. **f** Comparison of average monthly sedimentation.

https://doi.org/10.1038/s41467-025-57891-7

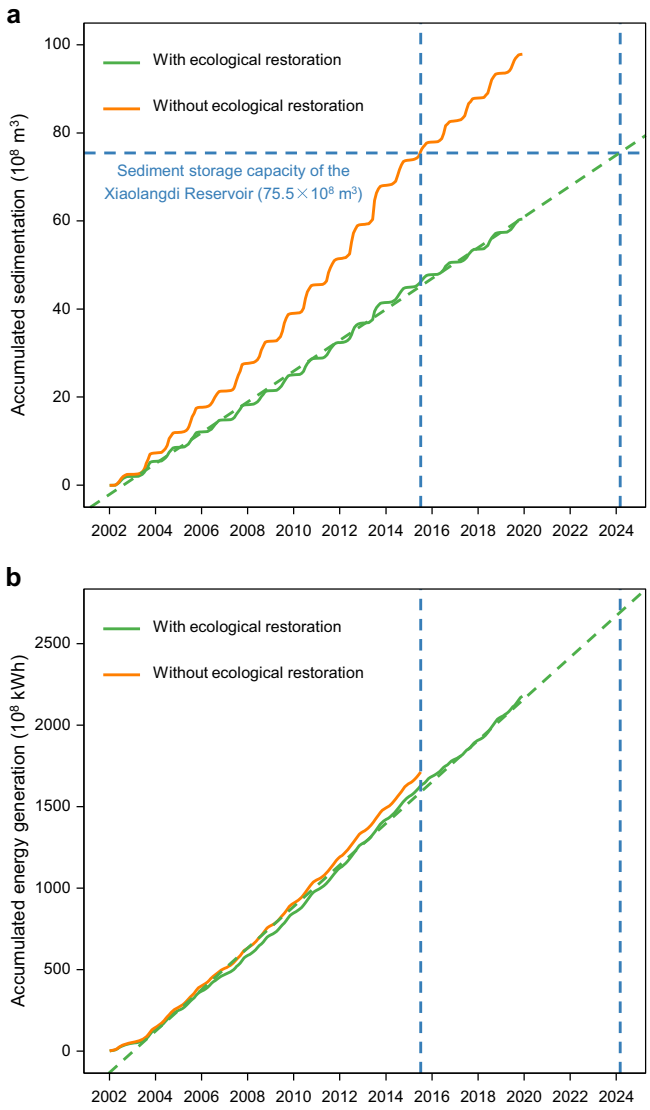

Fig. 5 | Accumulated sedimentation and energy generation of the Xiaolangdi Reservoir under scenarios with and without ecological restoration. **a** Accumulated sedimentation. **b** Accumulated energy generation.

and soil desiccation in certain areas and streamflow reduction of the YR due to the conflict between plant growth and water consumption[20,30,34]. The net positive impact of ER on hydropower potential is mainly attributed to the distinct sources of water and sediment of the YR. The water primarily originates upstream of Lanzhou, contributing about 60% of the annual runoff from less than 30% of the basin area[36], while nearly 90% of the sediment comes from the middle reaches, the Loess Plateau, which suffered severe soil erosion due to historical deforestation and agricultural development[37]. Since large-scale ER was mainly implemented in the middle YRB (Fig. 1, Supplementary Figs. 4 and 5), the reduction in sediment load into the Xiaolangdi Reservoir is disproportionately higher than the reduction in streamflow. Consequently, the negative impact of ER on hydropower through reduced annual energy generation is offset by the significant reduction in reservoir sedimentation. Beyond the focus on energy production in this study, the Xiaolangdi Reservoir provides other critical socioeconomic benefits, including flood and ice jam control, agricultural irrigation, and the regulation of seasonal water supply to meet the demands of cities and villages along the lower YR[32]. Since these functions depend on effective storage capacity, their reliability is also affected by reservoir sedimentation[16]. The sediment load reduction achieved through ER mitigates sedimentation, enhancing the security of energy, food, and environment[17]. However, the broader impacts of ER on these benefits require further exploration, integrating hydrological and sediment changes as demonstrated in this study.

Sediment is a fundamental challenge for hydropower development[17], with reservoirs worldwide losing storage capacity much faster than expected due to climate change and human activities[16]. For example, reservoirs in the upper Yangtze River, China's largest hydropower production region, have been affected by increasing sediment flux from the headwaters in recent decades[16]; the Tarbela Reservoir in the Indus River, Pakistan's largest hydropower and irrigation project, lost ~30% of its original storage capacity between 1974 and 2006, far exceeding initial expectations[38]; the Manwan and Dachaoshan Dams in the Mekong River have lost over 50% of their storage capacity because of sediment accumulation[9]; the Jirau and Santo Antonio Dams in the Madeira River have had to use dredgers to remove sediment accumulating at unexpected rates within five years of their completion[15]. As reservoirs are usually constructed at the most viable sites, their storage capacity loss to sedimentation is challenging to offset by building new ones[14]. The experiences from the YR can be extended to other rivers worldwide to mitigate reservoir sedimentation and enhance hydropower potential through rational watershed land use management. While controlling erosion at its source is widely recommended, it remains poorly implemented in reservoir sediment management due to the lack of direct benefits for land users[39]. In the YRB, ER was primarily funded by China's central and local governments[31] and separated from the construction of the Xiaolangdi Reservoir, yet it yielded the unintended but beneficial outcome of enhanced hydropower potential. This bonus benefit highlights the feasibility of payment for ecosystem services (PES) in other rivers with hydropower and clarifies who should bear the cost. If simulations of the ecosystem-water-sediment-energy nexus for other rivers indicate that effective upstream land use management can increase energy generation from certain existing or planned reservoirs, hydropower companies could allocate a portion of their additional profits to compensate upstream communities for adopting sediment-reducing land use measures. Drawing on real-world practices in the YRB, these measures include converting cropland to terraces, forests, or grasslands, planting vegetation in landslide-prone areas, constructing check dams, and removing excess sediment from these dams[20]. By achieving targeted sediment load reductions through such measures, upstream farmers could receive compensation in the form of cash payments or rewards such as reduced energy costs from hydropower companies. Such PES mechanisms have proven successful in some small watersheds like Indonesia's Way Besai watershed[40]. As our study demonstrates their significant potential for large-scale integrated watershed management, they merit further expansion worldwide.

Besides the positive impact of ER on hydropower potential, our results also highlight the significant contributions of other sediment management measures. By the end of 2019, the accumulated sedimentation in the Xiaolangdi Reservoir was 97.91×10^8 m^3 under the scenario without ER and 60.43×10^8 m^3 with ER, compared to the observed value—representing the actual scenario with all influencing factors, including ER—of just 32.97×10^8 m^3. This indicates that ER accounted for 57.7% of the actual sedimentation reduction of 64.94×10^8 m^3, with the remaining 42.3% attributed to other measures not included in our simulations. These measures likely involve reservoir operations such as sediment bypassing, sluicing, dredging, and drawdown flushing[41], as well as the complex water and sediment regulation scheme (WSRS) of the YR[28,32]. The WSRS, a coordinated regulation of three major reservoirs (Wanjiazhai, Sanmenxia, and Xiaolangdi) along the YR mainstream[42], is generally operated every summer to enhance sediment delivery by unleashing artificial flood waves. Together with ER in the YRB, the WSRS has greatly extended the life expectancy of the Xiaolangdi Reservoir's sediment storage

capacity, which was initially projected to be exhausted by 2020. Such coordinated reservoir regulation provides a promising complement to watershed PES and could be applied to other rivers with cascade reservoirs, such as the Yangtze, Nile, and Mekong. Effective operation of cascade reservoirs requires two regulation phases: in the first phase, clear water is released from the downstream reservoir to lower its water level; in the second phase, floodwaters from the coordinated operation of upstream reservoirs scour previously deposited sediment in the downstream reservoir, generating an artificial hyperpycnal flow with high sediment concentration and fluid density[42]. In this way, sedimentation of downstream reservoirs can be effectively mitigated.

As this study primarily focuses on determining whether the net impact of ER on hydropower potential is positive or negative, rather than accurately simulating real hydropower production, several simplifications and compromises were made in the experimental design. First, the estimated hydropower represents the potential of the Xiaolangdi Reservoir in the absence of upstream reservoirs' operations and socioeconomic water use. Simulating the long-term operations of upstream reservoirs and socioeconomic water use is challenging. These processes depend on upstream streamflow and sediment load. If included in the scenarios, these processes would vary in tandem with changes in upstream streamflow and sediment load driven by ER, rather than remaining consistent across different scenarios, making it complex and difficult to isolate the impact of ER. Our simplification ensures that differences between scenarios reflect the hydrological and sediment responses attributable solely to ER, although it limits direct comparability with real-world gauge observations. In practice, upstream reservoirs' operations and socioeconomic water use reduce the actual streamflow and sediment load entering the Xiaolangdi Reservoir compared to our ER simulation (Supplementary Fig. 6). Although this results in lower average annual energy generation and sedimentation in reality, the relationship between accumulated sedimentation and energy generation suggests that the actual accumulated hydropower production may exceed our simulations (Supplementary Fig. 7). Second, large-scale land use change may indirectly influence hydropower potential by affecting precipitation, partially offsetting its impact on local water availability[23,43]. While this complex feedback between land use change and climate was not incorporated into our simulations—given prior findings that precipitation increase from vegetation greening was statistically insignificant in North China[44]—it remains an important consideration for future simulations in other regions. Third, sedimentation distributions, which affect reservoir storage, are shaped by complex hydrological and sediment processes, such as the movement of fine-grained sediment deposits[45]. Accurately modeling these processes over the long term remains challenging. Instead, we assumed that sediment initially accumulates at the reservoir's lowest elevation and gradually increases over time. This assumption implies that sedimentation occurs first in the sediment storage of the Xiaolangdi Reservoir (mainly below the water level of 245 m, Supplementary Fig. 2) and enables us to simulate changes in the relationship between storage and forebay water level as sedimentation accumulates. Although idealized, this assumption aligns reasonably well with daily storage and water level data spanning 2006 to 2023 ("Methods", Supplementary Fig. 8, Table 3). Fourth, sediment storage exhaustion was used as a benchmark to evaluate and compare total energy generation across scenarios; while it reduces reservoir flexibility and efficiency, power generation remains possible. Analysis of the relationship between accumulated sedimentation and energy generation (Supplementary Fig. 7) showed that, regardless of the storage threshold chosen as the benchmark, the scenario with ER consistently yielded higher energy output—generally exceeding 50% more—underscoring the robustness of our findings. These simplifications, while necessary for the scope of this study, may affect the precision of our results and should be addressed in future research to enhance accuracy and applicability.

In conclusion, this study revealed the positive impact of ER in the YRB on hydropower potential by integrating the opposing effects through sediment and runoff changes. It advances our understanding of the ecosystem-water-sediment-energy nexus and underscores the vital role of integrated watershed management in sustainable development. The insights from this study can be applied to other reservoirs worldwide, guiding PES practices in different watersheds.

Methods

Data sources

This study utilized various datasets to analyze and simulate the vegetation dynamics in the YRB, the streamflow and sediment concentration of the YR, and the regulation of the Xiaolangdi Reservoir (Supplementary Table 2). Meteorological variables, such as daily minimum, maximum, and mean temperatures, relative humidity, wind speed, solar radiation, and sunshine duration, were interpolated from data at 113 national meteorological stations distributed across or near the YRB, provided by the China Meteorological Administration (http://data.cma.cn). Precipitation data were sourced from the China Gauge-based Daily Precipitation Analysis (CGDPA), a 0.25° gridded daily dataset integrated from observations of 113 national meteorological stations and other undisclosed meteorological stations using the climatology-based optimal method detailed by Shen and Xiong[46]. Geographic and soil texture data for the YRB were obtained from the Shuttle Radar Topography Mission (SRTM) digital elevation model (DEM) by Jarvis et al.[47]. and the soil information database by Shangguan et al.[48]. The border and DEM data for the Xiaolangdi Reservoir were sourced from Li et al.[49]. Soil hydraulic parameters were obtained from Dai et al.[50]. Vegetation type data were collected from the investigative vegetation maps of China (1:1,000,000)[51,52] and the 30-m resolution Global Land Cover dataset[53,54]. ER construction records, including terracing, check dams, afforestation, and grass planting, were primarily collected from the Chinese National Water Resources Census (http://www.mwr.gov.cn/) and the Yellow River Conservancy Commission of the Ministry of Water Resources (http://www.yrcc.gov.cn/).

Comprehensive hydrological, ecological, and sediment datasets, such as Leaf Area Index (LAI), Gross Primary Productivity, evapotranspiration, etc., were employed for model calibration and validation. Specifically, this study aimed to simulate streamflow and sediment load without the influence of other reservoirs' operations and socioeconomic water use upstream of the Xiaolangdi Reservoir. To this end, hydrological processes were first calibrated and validated using natural streamflow sequences from 1982 to 2000, obtained from the third national water resources survey and evaluation conducted by the Ministry of Water Resources (http://www.mwr.gov.cn/). This dataset restored surface water consumption, reservoir operations, and evaporation and leakage caused by the reservoirs, based on gauge observations. After establishing reliable hydrological modeling, sediment load was then calibrated and validated using observed sediment load from 1960 to 1980, during which most reservoirs on the YR had not yet been constructed, to approximate sediment processes without the influence of reservoir sedimentation. Observed sediment load data, along with data on the regulation and storage of the Xiaolangdi Reservoir, were provided by the Yellow River Conservancy Commission of the Ministry of Water Resources (http://www.yrcc.gov.cn/). More details on these datasets and their processing for simulating and validating vegetation, runoff, and sediment can be found in Yan et al.[19,55] and Yang et al.[56].

Simulation of streamflow and sediment load of the YR

The Geomorphology-Based Eco-hydrological Model with Soil and Water Conservation (GBEHM-SWC), a distributed physically-based eco-hydrological model, was used to simulate hydrological and sediment dynamics under varying vegetation cover and engineering conditions. The Geomorphology-Based Eco-hydrological Model (GBEHM)[57], integrates a comprehensive set of processes, including

hydrological dynamics governed by multi-layer soil water dynamics and energy balance, and erosion processes on hillslopes influenced by underlying surface characteristics and the hydraulic properties of overland flow. Furthermore, the model simulates kinematic wave flow routing and one-dimensional non-equilibrium sediment transport in river channels, offering a holistic representation of eco-hydrological interactions across both hillslope and channel systems (Supplementary Fig. 3). Developed from GBEHM, the GBEHM-SWC has been further refined to capture the impacts of soil and water conservation measures (ER measures in this study) on hydrological and sediment processes[19]. These measures are explicitly represented to depict their hydrological and sediment influences in the GBEHM-SWC. Terracing, afforestation, and grass planting on hillslopes first alter vegetation cover—a change observable through remote-sensed LAI data. They are also parameterized to enhance surface water storage capacity and reduce erosion capacity, integrated into hillslope hydro-sediment processes. Check dams in the river network system are conceptualized as unregulated reservoirs within each flow interval and incorporated into the flow routing process. These dams slow down discharge velocity or obstruct streamflow to facilitate sediment deposition, with stored water further infiltrating or evaporating. The outflow discharge and sediment concentration are calculated based on the simulated inflow and effective storage capacity of check dams, while dynamically tracking changes in water storage and sediment deposition within the dams. The parameterization scheme is detailed in Yan et al.[19] and Yang et al.[56]. The GBEHM-SWC was extensively calibrated and validated in the YRB using monthly natural streamflow data from 38 hydrological stations and monthly observed sediment discharge data from 22 hydrological stations, demonstrating advanced performance with Nash-Sutcliffe efficiency coefficient (NSE) values for streamflow exceeding 0.8 (Supplementary Fig. 9) and NSE values for sediment discharge exceeding 0.5 at all mainstream stations (Supplementary Fig. 10).

Scenario analysis of ER impacts on energy generation of the Xiaolangdi Reservoir

We employed a single-factor fixed approach to assess the impacts of ER in the YRB on water and sediment changes of the YR and subsequently on the energy generation of the Xiaolangdi Reservoir. The scenario with ER represented current conditions with all restoration practices in place, while the scenario without ER reflected the pre-restoration landscape of the YRB (Supplementary Table 1). ER measures in the YRB, aimed at controlling severe soil erosion and reducing sediment transport, include terracing, afforestation, grass planting on hillslopes, and check dams in the river network. For the scenario with ER, actual ER measures from 2000 to 2019 and dynamic land use and LAI were used as inputs. The streamflow and sediment discharge into the Xiaolangdi Reservoir simulated by the GBEHM-SWC under this scenario showed high consistency with observed data from 2000 to 2019, with R^2 values of 0.70 and 0.53 and NSE values of 0.67 and 0.45 for monthly natural streamflow and sediment discharge, respectively (Supplementary Figs. 11 and 12). In the scenario without ER, no ER measures were applied, and only the land use in 2000 and simulated natural vegetation dynamics based on the Biome-BGC model (Supplementary Fig. 13) were used as inputs.

The Biome-BGC model, a widely recognized tool for simulating vegetation ecophysiology, models the processes of energy, water, and carbon fluxes within terrestrial ecosystems and provides key variables like LAI. We used version 4.2 of the Biome-BGC model, which has been extensively validated and widely employed in previous studies[58,59], to simulate the vegetation condition of the YRB from 2000 to 2019, accounting only for climatic influences and excluding human interference. The model was adapted to simulate vegetation dynamics on a 10-km grid cell scale, matching the spatial resolution of the eco-hydrological model. The NSE values for simulated monthly LAI for all vegetation types at five sample grids exceeded 0.85, averaging 0.90, demonstrating satisfactory performance. After calibrating the model parameters at the sample points, the Biome-BGC model was run for each grid. More details on the simulation process can be found in Yan et al.[55].

Simulation of energy generation and sedimentation of the Xiaolangdi Reservoir

A random forest model was used to simulate the regulation rules of the Xiaolangdi Reservoir. Reservoir operation is typically based on its storage, purpose, and inflow[60], and shows monthly variations attributed to seasonal inflow patterns, downstream irrigation water demands, and hydropower generation necessities[61]. Therefore, the monthly outflow released from the reservoir (O_t, m^3/s) was predicted using the storage at the beginning of the month (S_t, 10^8 m^3), the inflow of the month (I_t, m^3/s) and the month before (I_{t-1}, m^3/s), and the month itself (t) as explanatory variables. We used monthly regulation data of the Xiaolangdi Reservoir from June 2006 to March 2024 to build the model, with 80% of the data randomly selected for training and the remaining 20% for validation. The model showed high accuracy with NSE values of 0.88, 0.77, and 0.86 and R^2 values of 0.94, 0.79, and 0.91 for training, validation, and all data, respectively (Supplementary Figs. 14 and 15).

Using the regulation rules model and hydrological and sediment output from the GBEHM-SWC, we simulated the regulation of the Xiaolangdi Reservoir under scenarios with and without ER (Supplementary Fig. 16). The simulation began in January 2002, following the completion of the reservoir construction at the end of 2001, with an initial recorded storage of 4.5 billion m^3. The simulated storage was calculated using the water balance of the reservoir as Eq. (1):

$$S_{t+1} = S_t + (I_t - O_t)\cdot \Delta t / 10^8 \quad (1)$$

where Δt is the total seconds of the corresponding month for each step size. To better reflect real-world reservoir regulation, we added two constraints: the maximum simulated storage should be less than the storage capacity at the simulated time, calculated as the initial storage capacity (12.65 billion m^3) minus the accumulated sedimentation; the minimum simulated storage should be higher than the lowest values observed in the actual regulation of the reservoir (0.05 billion m^3).

Based on simulated sediment concentration of the inflow into the Xiaolangdi Reservoir and outflow and storage of the reservoir, monthly energy generation and sedimentation of the Xiaolangdi Reservoir were calculated. According to a previous study[62], the electricity generated by the Xiaolangdi Reservoir was calculated as Eq. (2):

$$E_t = K \cdot O'_t \cdot (H_t - H_0) \cdot \Delta t / 3600 \quad (2)$$

where E_t is the generated electricity (kWh); K is the power generation coefficient (8.5 for large hydropower stations)[62]; O'_t is the water released for power generation, generally equal to O_t but capped at 1800 m^3/s, the maximum flow rate that the turbine can handle[62]; H_t is the average fore-bay water level during month t, and H_0 is the turbine layer elevation (129 m)[62]. H_t was calculated based on the average storage during month t and a quadratic polynomial function fitted to the relationship curve between storage and fore-bay water level of the Xiaolangdi Reservoir. The initial relationship was derived using DEM data (Supplementary Figs. 8 and 17). This relationship evolves with sedimentation in the Xiaolangdi Reservoir. Given the challenges in accurately predicting sedimentation distributions, we assumed that sediment initially accumulates at the reservoir's lowest elevation and gradually increases over time. Consequently, as the reservoir silts up, changes in the storage–water level relationship curve are primarily reflected in shifts in the intercept. The relationship function was recalculated annually during the simulation. We validated our assumption using daily storage and water level data of the Xiaolangdi

Reservoir spanning 2006–2023. Data points from different years demonstrated similar curvature to the initial relationship (Supplementary Fig. 8a). Additionally, the fitting functions for the storage–water level relationship, derived from the initial function with adjusted intercepts for all years, showed high R^2 values exceeding 0.99 (Supplementary Table 3). The changes in the fitting function intercept and the changes in actual accumulated reservoir sedimentation over different years exhibit an inverse relationship (Supplementary Fig. 8b), indicating that the reduction in storage at any given water level is nearly equal in magnitude to the sedimentation during those years. This consistency supports the robustness of our assumption that sediment initially accumulates at the reservoir's lowest elevation.

To calculate reservoir sedimentation, the sediment concentration of the outflow was derived using an empirical formula for the sediment delivery ratio of the Xiaolangdi Reservoir established in a previous study[63]. This formula characterizes the relationship between the sediment delivery ratio and its influencing factors—including average storage, outflow, inflow, and inflow sediment concentration of the Xiaolangdi Reservoir—as Eq. (3) and exhibits a high fitting accuracy ($R^2 = 0.86$) with observed data from 2000 to 2015 (Supplementary Fig. 18):

$$\eta_t = 1.493 \cdot (\bar{S}_t/O_t)^{-1.008} \cdot (I_t/O_t)^{-0.278} \cdot ScI_t{}^{-0.404} \quad (3)$$

therefore, the sediment concentration of the outflow can be expressed as Eq. (4):

$$ScO_t = \eta_t \cdot ScI_t \cdot I_t/O_t \quad (4)$$

where η_t is the sediment delivery ratio; $\bar{S}_t$ is the average storage during month t (10^8 m^3); ScI_t and ScO_t are the sediment concentrations of the inflow and outflow, respectively (kg/m^3). Using the mass conservation equation, the reservoir sedimentation volume can be calculated as Eq. (5):

$$\Delta V_t = (I_t \cdot ScI_t - O_t \cdot ScO_t) \cdot \Delta t/\rho \quad (5)$$

where ΔV_t is the sedimentation volume of the reservoir in month t (m^3); ρ is the dry density of the bed sediment, taken as 1200 kg/m^3.

Data availability

All the data used in this study can be obtained from the sources listed in Supplementary Table 2.

Code availability

All computer codes used in this study are available from the corresponding author upon request.

References

1. United Nations. Transforming our world: The 2030 agenda for sustainable development. *General Assembley 70* Session (United Nations, 2015).
2. IRENA. *Renewable Capacity Statistics 2024* (International Renewable Energy Agency, Abu Dhabi, 2024).
3. Carlino, A. et al. Declining cost of renewables and climate change curb the need for African hydropower expansion. *Science* **381**, eadf5848 (2023).
4. Gernaat, D. E. H. J., Bogaart, P. W., Vuuren, D. P. V., Biemans, H. & Niessink, R. High-resolution assessment of global technical and economic hydropower potential. *Nat. Energy* **2**, 821–828 (2017).
5. Xu, R. et al. A global-scale framework for hydropower development incorporating strict environmental constraints. *Nat. Water* **1**, 113–122 (2023).
6. Sterl, S. et al. Smart renewable electricity portfolios in West Africa. *Nat. Sustain* **3**, 710–719 (2020).
7. Fan, P. et al. Recently constructed hydropower dams were associated with reduced economic production, population, and greenness in nearby areas. *Proc. Natl. Acad. Sci. USA* **119**, e2108038119 (2022).
8. IRENA. *The Changing Role of Hydropower: Challenges and Opportunities* (International Renewable Energy Agency, Abu Dhabi, 2023).
9. Chua, S. D. X. et al. Can restoring water and sediment fluxes across a mega-dam cascade alleviate a sinking river delta? *Sci. Adv.* **10**, eadn9731 (2024).
10. Chowdhury, A. F. M. K. et al. Hydropower expansion in eco-sensitive river basins under global energy-economic change. *Nat. Sustain.* **7**, 213–222 (2024).
11. Zarfl, C., Lumsdon, A. E., Berlekamp, J., Tydecks, L. & Tockner, K. A global boom in hydropower dam construction. *Aquat. Sci.* **77**, 161–170 (2015).
12. Schleiss, A. J., Franca, M. J., Juez, C. & De Cesare, G. Reservoir sedimentation. *J. Hydraul. Res.* **54**, 595–614 (2016).
13. Ran, L., Lu, X. X., Xin, Z. & Yang, X. Cumulative sediment trapping by reservoirs in large river basins: a case study of the Yellow River basin. *Global Planet. Change* **100**, 308–319 (2013).
14. Perera, D., Williams, S. & Smakhtin, V. Present and future losses of storage in large reservoirs due to sedimentation: a country-wise global assessment. *Sustainability* **15**, 219 (2023).
15. Moran, E. F., Lopez, M. C., Moore, N., Muller, N. & Hyndman, D. W. Sustainable hydropower in the 21st century. *Proc. Natl. Acad. Sci. USA* **115**, 11891–11898 (2018).
16. Li, D. et al. Exceptional increases in fluvial sediment fluxes in a warmer and wetter High Mountain Asia. *Science* **374**, 599–603 (2021).
17. Li, D. et al. High Mountain Asia hydropower systems threatened by climate-driven landscape instability. *Nat. Geosci.* **15**, 520–530 (2022).
18. Chung, M. G., Frank, K. A., Pokhrel, Y., Dietz, T. & Liu, J. Natural infrastructure in sustaining global urban freshwater ecosystem services. *Nat. Sustain.* **4**, 1068–1075 (2021).
19. Yan, Z. et al. Simulating the hydrological impacts of intensive soil and water conservation measures in the Yellow River basin using a distributed physically-based model. *J. Hydrol.* **625**, 129936 (2023).
20. Fu, B. et al. Hydrogeomorphic ecosystem responses to natural and anthropogenic changes in the Loess Plateau of China. *Annu. Rev. Earth Planet. Sci.* **45**, 223–243 (2017).
21. Xi, Y. et al. Trade-off between tree planting and wetland conservation in China. *Nat. Commun.* **13**, 1967 (2022).
22. Zhang, M. & Wei, X. Deforestation, forestation, and water supply. *Science* **371**, 990–991 (2021).
23. Stickler, C. M. et al. Dependence of hydropower energy generation on forests in the Amazon Basin at local and regional scales. *Proc. Natl. Acad. Sci. USA* **110**, 9601–9606 (2013).
24. de Oliveira Serrão, E. A. et al. Land use change scenarios and their effects on hydropower energy in the Amazon. *Sci. Total Environ.* **744**, 140981 (2020).
25. Vogl, A. L. et al. Managing forest ecosystem services for hydropower production. *Environ. Sci. Policy* **61**, 221–229 (2016).
26. Vogl, A. L. et al. Valuing investments in sustainable land management in the Upper Tana River basin, Kenya. *J. Environ. Manage.* **195**, 78–91 (2017).
27. Wang, S. et al. Reduced sediment transport in the Yellow River due to anthropogenic changes. *Nat. Geosci.* **9**, 38–41 (2016).
28. Best, J. Anthropogenic stresses on the world's big rivers. *Nat. Geosci.* **12**, 7–21 (2019).
29. Wang, G., Wu, B. & Wang, Z. Y. Sedimentation problems and management strategies of sanmenxia reservoir, yellow river, china. *Water Resour. Res.* **41**, W09417 (2005).
30. Feng, X. et al. Revegetation in China's Loess Plateau is approaching sustainable water resource limits. *Nat. Clim. Change* **6**, 1019–1022 (2016).

31. Wu, X., Wang, S., Fu, B., Feng, X. & Chen, Y. Socio-ecological changes on the Loess Plateau of China after Grain to Green Program. *Sci. Total Environ.* **678**, 565–573 (2019).
32. Kong, D. et al. Environmental impact assessments of the Xiaolangdi Reservoir on the most hyperconcentrated laden river, Yellow River, China. *Environ. Sci. Pollut. Res.* **24**, 4337–4351 (2017).
33. Yellow River Conservancy Commission of the Ministry of Water Resources. *Soil and Water Conservation Bulletin in Yellow River Basin 2020* (In Chinese) (Yellow River Conservancy Commission of the Ministry of Water Resources, 2022).
34. Fu, B., Wu, X., Wang, Z., Wu, X. & Wang, S. Coupling human and natural systems for sustainability: experience from China's Loess Plateau. *Earth Syst. Dyn.* **13**, 795–808 (2022).
35. Liu, Y. et al. Recent anthropogenic curtailing of Yellow River runoff and sediment load is unprecedented over the past 500 y. *Proc. Natl. Acad. Sci. USA* **117**, 18251–18257 (2020).
36. Yang, D., Yang, Y., Gao, G., Huang, J. & Jiang, E. Water cycle and soil-water coupling processes in the Yellow River Basin. *Bull. Natl. Nat. Sci. Found. China* **35**, 544–551 (2021).
37. Wu, X. et al. Evolution and effects of the social-ecological system over a millennium in China's Loess Plateau. *Sci. Adv.* **6**, eabc0276 (2020).
38. Annandale, G. W., Morris, G. L., Karki, P. *Extending the Life of Reservoirs: Sustainable Sediment Management for Dams and Run-of-river Hydropower* (World Bank Group, 2016).
39. Morris Gregory, L., Annandale, G., Hotchkiss, R. Reservoir sedimentation. In *Sedimentation Engineering: Processes, Measurements, Modeling, and Practice* (American Society of Civil Engineers, Reston, Virginia, U.S., 2008).
40. UNEP. *Nature-based Solutions to Emerging Water Management Challenges in the Asia-Pacific Region* (United Nations Environment Programme, Nairobi, 2022).
41. Kondolf, G. M. et al. Sustainable sediment management in reservoirs and regulated rivers: experiences from five continents. *Earth's Future* **2**, 256–280 (2014).
42. Wang, H. et al. Impacts of the dam-orientated water-sediment regulation scheme on the lower reaches and delta of the Yellow River (Huanghe): a review. *Global Planet Change* **157**, 93–113 (2017).
43. Hoek van Dijke, A. J. et al. Shifts in regional water availability due to global tree restoration. *Nat. Geosci.* **15**, 363–368 (2022).
44. Li, Y. et al. Divergent hydrological response to large-scale afforestation and vegetation greening in China. *Sci. Adv.* **4**, aar4182 (2018).
45. Jia, D., Wang, Y., Jiang, E., Shao, X. & Zhang, X. Numerical study on the sedimentation pattern of Xiaolangdi Reservoir on the Yellow River. *Adv. Water Sci.* **31**, 240–248 (2020). In Chinese.
46. Shen, Y. & Xiong, A. Y. Validation and comparison of a new gauge-based precipitation analysis over mainland China. *Int. J. Climatol.* **36**, 252–265 (2016).
47. Jarvis, A. Hole-filed seamless SRTM data. http://srtm.csi.cgiar.org (2008).
48. Shangguan, W., Dai, Y. J., Duan, Q. Y., Liu, B. Y. & Yuan, H. A global soil data set for earth system modeling. *J. Adv. Model. Earth Sy.* **6**, 249–263 (2014).
49. Li, Y., Gao, H., Zhao, G. & Tseng, K.-H. A high-resolution bathymetry dataset for global reservoirs using multi-source satellite imagery and altimetry. *Remote Sens. Environ.* **244**, 111831 (2020).
50. Dai, Y. J. et al. Development of a China dataset of soil hydraulic parameters using pedotransfer functions for land surface modeling. *J. Hydrometeorol.* **14**, 869–887 (2013).
51. Zhang, X. *Vegetation Map of the People's Republic of China (1:1 000 000 000)* (Geology Press, 2007).
52. Su, Y. J. et al. An updated Vegetation Map of China (1:1000000). *Sci. Bull.* **65**, 1125–1136 (2020).
53. Zhang, X. et al. Development of a global 30m impervious surface map using multisource and multitemporal remote sensing datasets with the Google Earth Engine platform. *Earth Syst. Sci. Data* **12**, 1625–1648 (2020).
54. Zhang, X. et al. GLC_FCS30: global land-cover product with fine classification system at 30m using time-series Landsat imagery. *Earth Syst. Sci. Data* **13**, 2753–2776 (2021).
55. Yan, Z., Wang, T., Ma, T. & Yang, D. Water-carbon-sediment synergies and trade-offs: Multi-faceted impacts of large-scale ecological restoration in the Middle Yellow River Basin. *J. Hydrol.* **634**, 131099 (2024).
56. Yang, H. et al. Runoff and sediment effect of the soil-water conservation measures in a typical river basin of the Loess Plateau. *Catena* **243**, 108218 (2024).
57. Yang, D. et al. A distributed scheme developed for eco-hydrological modeling in the upper Heihe River. *Sci. China Earth Sci.* **58**, 36–45 (2015).
58. Thornton, P. E. et al. Modeling and measuring the effects of disturbance history and climate on carbon and water budgets in evergreen needleleaf forests. *Agric. Meteorol.* **113**, 185–222 (2002).
59. Chiesi, M. et al. Application of BIOME-BGC to simulate Mediterranean forest processes. *Ecol. Modell.* **206**, 179–190 (2007).
60. Hanasaki, N., Kanae, S. & Oki, T. A reservoir operation scheme for global river routing models. *J. Hydrol.* **327**, 22–41 (2006).
61. Wang, Z. et al. A generalized reservoir module for SWAT applications in watersheds regulated by reservoirs. *J. Hydrol.* **616**, 128770 (2023).
62. Xia, J., Chen, Y., Deng, S., Zhou, M. & Wang, Z. Coupled modeling of flow–sediment transport and power generation in the Xiaolangdi Reservoir. *Adv. Eng. Sci.* **53**, 113–121 (2021).
63. Zhang, S., Xia, J. & Li, T. Study on flood-season sediment delivery ratio of the Xiaolangdi Reservoir. *Yellow River* **40**, 7–11 (2018).

Acknowledgements

This research was financially supported by the National Natural Science Foundation of China (42041007, B.F. and S.W.; 42430505, B.F. and X.W.; 42201306, X.W.). We thank Dr. Jieyu Li from the Yellow River Institute of Hydraulic Research, Yellow River Conservancy Commission, for providing information on the Xiaolangdi Reservoir.

Author contributions

X.W. and S.W. designed the research. Z.Y. and H.Y. contributed to the simulation of streamflow and sediment load of the Yellow River. X.W. and Y.S. contributed to the simulation of regulation of the Xiaolangdi Reservoir. X.W., Z.Y., H.Y., and H.Z. performed the data analysis. The manuscript was drafted by X.W. and edited by Z.Y., H.Y., S.W., H.Z., Y.S., S.S., Y.L., Y.G., D.Y., and B.F.

Competing interests

The authors declare no competing interests.

Additional information

Supplementary information The online version contains supplementary material available at https://doi.org/10.1038/s41467-025-57891-7.

Correspondence and requests for materials should be addressed to Shuai Wang.

Peer review information *Nature Communications* thanks Alban Kuriqi, Yinjun Zhou and the other, anonymous, reviewer for their contribution to the peer review of this work. A peer review file is available.